IEEE Access
Multidisciplinary | Rapid Review | Open Access Journal

Received March 19, 2020, accepted March 28, 2020, date of publication April 6, 2020, date of current version June 1, 2020.

Digital Object Identifier 10.1109/ACCESS.2020.2986040

Single-Layer Dual-Band Wide Band-Ratio Reflectarray With Orthogonal Linear Polarization

XI LI, (Member, IEEE), XI LI, AND LIN YANG
National Laboratory of Science and Technology on Antennas and Microwaves, Xidian University, Xi'an 710071, China
Corresponding author: Xi Li (xlixidian@163.com)

ABSTRACT In this letter, a single-layer broadband wide band-ratio (ratio of f_{higher} to f_{lower}) reflectarray that can achieve different linear polarizations at the X-band and the K-band is designed. Its elements consist of a split square loop with two square shaped phase delay lines (outer structure) and a phoenix square loop (inner structure) operating at the X-band and the K-band, respectively. The ingeniousness of the design is that the outer structure and the inner structure can achieve a $0^\circ - 360^\circ$ phase shift by adjusting the phase shift lines and the side length of the inner square ring, respectively. At the same time, they do not affect each other in space. Different polarizations corresponding to the two structures are orthogonal to each other, so their electrical performances do not affect each other. To verify our design concept, the reflectarray is fabricated and measured in a microwave anechoic chamber. The simulated and measured results are in good agreement. The measured gains are 23.6 dBi at 10 GHz (f_{lower}) with aperture efficiency of 48%, and 30.6 dBi at 22 GHz(f_{higher}) with aperture efficiency of 43%. The 1-dB gain bandwidths are 20% (9.1 GHz–11.1 GHz) at the X-band and 19% (19.8 GHz–23.9 GHz) at the K-band. The band-ratio of the reflectarray is 2.2. A single-layer dual-band wide band-ratio reflectarray with dual-linear polarization is confirmed.

INDEX TERMS Double linear polarization, reflectarray, single-layer, wide band-ratio.

I. INTRODUCTION

As a new kind of high-gain antenna, a reflectarray antenna has the advantages of a simple structure, low cost, simple feed network, flexible beam control, and so on. It can be widely used in long-distance wireless communication, electronic countermeasures, and radar detection [1]. It effectively combines the advantages of a reflector antenna and a planar microstrip array antenna.

With the development of communication technologies, there is an increasing demand for dual-frequency or multi-frequency antennas, especially broadband wide band-ratio dual-band antennas. In practical applications, broadband wide band-ratio dual-band antennas (such as X- and K-bands) are often used in satellite communications. By using one reflectarray and two feeds operating at different bands, the satellite communication requirements can be significantly lowered, which provides cost reductions. [2]. At present, dual-band reflectarrays are mainly implemented in two ways. The first uses two different resonance elements on a single-layer dielectric substrate, and they work at different bands [3]–[12]. The second consists of a multilayer dielectric plate [13]–[15], and the different resonant elements operating at distinct bands are on separate dielectric layers. In the first case, the different kinds of elements operate at each polarization independently. For example, two kinds of elements are alternately distributed on a plane [3]. In order to reduce the coupling between the higher-band and the lower-band, the dual-band frequency selective surface (FSS) is used instead of a reflective ground plane. This approach reduces the interference between the two bands, but the aperture efficiency of the reflectarray also drops dramatically. In [4], a single-layer dual-band linear plane reflection array is proposed. The phase responses corresponding to different bands are determined by a variable. Because there is a certain relationship between the beam directions corresponding to the two bands, it is not possible to make the beams corresponding to the two frequencies point to any direction casually. In addition, the antenna cannot be applied in practice at high frequencies due to its low aperture efficiency. A single-layer dual-band circularly polarized reflectarray has been designed [5]. The proposed approach combines two kinds of elements operating at different bands to make full use of the space. However, its high-frequency element can only

The associate editor coordinating the review of this manuscript and approving it for publication was Yingsong Li.

achieve a 300° phase shift, so its cross-polarization and the side-lobe level are relatively high. A low-cost single layer metal-only reflectarray antenna operating at X/Ku dual-band is proposed [6]. It has a higher aperture efficiency for its metal-only structure, but the weight is large, and the band-ratio is 1.5. In the second case, a reflectarray based on three stacked layers of varying-sized patches is described, which can realize dual-frequency radiation. However, the complicated structure makes the processing cost high [13] [14]. There are many ways to decouple the bands. A five-band tunable terahertz metamaterial absorber composed of an absorbing layer, a metal layer, and a dielectric layer is proposed in [18]. However, as the incident frequency increases, the resonant mode of the absorber also changes. In this paper, the proposed cell is decoupled by a two-part structure corresponding to different orthogonal linear polarizations.

Up to now, the band-ratio of the single-layer dual-band reflectarray is generally less than two. For two different kinds of elements, the distribution of the elements corresponding to wide band-ratio bands is difficult to achieve, which causes higher side lobes and higher cross polarization. Grating lobes will be generated if the distance between high-frequency elements is too large, so it is difficult to achieve a single-layer dual-band wide band-ratio reflectarray. In this article, the novel element we design consists of two parts: the phoenix square loop corresponds to the K-band, and the split square loop with two square shaped phase delay lines corresponds to the X-band. The ingeniousness of the design is that outer structure's phase shift lines and the inner structure's side length can be adjusted to achieve a 0°-360° phase shift. At the same time, the structures do not affect each other in space. Different polarizations corresponding to the outer structure and the inner structure are orthogonal to each other, so their electrical performances are independent. As far as the author knows, this is the widest frequency ratio in a single layer dual-band reflectarray, and the 1-dB gain bandwidths can reach almost 20% in both bands.

II. PROPOSED ELEMENT CONSTRUCTION AND DUAL-BAND REFLECTION PERFORMANCE

A. ELEMENT CONSTRUCTION

The proposed element, illustrated in Fig. 1(a), consists of two parts: the internal structure is a phoenix square loop operating at the K-band and the outer structure is a split square ring with two phase modulation lines which operate at the X-band. The elements are printed on one side of a dielectric substrate. It has the relative permittivity of $\varepsilon_r = 3.5$, loss tangent of $\delta = 0.0027$, and thickness of $h_1 = 1mm$. There is a 2 mm thick air layer between the dielectric substrate and the metal ground (GND) as shown in Fig. 1(b), which makes the reflection phase change more smoothly with the parameters of the element. The outermost dimensions of this element are 9 mm ($0.3\lambda_{lower}$ at 10 GHz and $0.66\lambda_{higher}$ at 22 GHz).

As shown in the Fig. 1(a), the external structure parameters affecting the reflection characteristics of the element are the

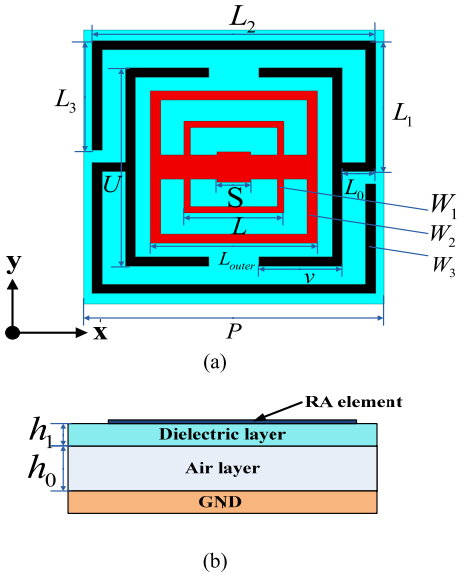

FIGURE 1. Construction of the element. (a) Front view of the element. (b) Side view of element.

total length of L2 and L3 (L2+L3) at 10 GHz. The range of L2+L3 is 1 mm-12 mm. The corresponding reflection magnitude is less than −0.3 dB as shown in Fig. 2(a); the corresponding phase of the reflection is 0° − 360° as shown in Fig. 2(c). The parameter affecting the reflection phase at 22 GHz in the internal structural is L, and the range of L is 1 mm-5 mm. The corresponding reflection magnitude is less than -0.3 dB as shown in Fig. 2(b); the corresponding phase of the reflection is 0° − 360° as shown in Fig. 2(d). The element can achieve a 0° − 360° phase shift of the reflection phase in both bands. This satisfies the basic requirements of a general reflectarray element, so that the reflectarray can achieve higher gain and lower sidelobe characteristics in dual bands. The detailed dimension parameters of the proposed element are given in Table 1; these are obtained through simulation and optimization.

B. ANALYSIS OF INTERACTION BETWEEN HIGHER AND LOWER BAND ELEMENT

For a reflectarray, the adjustment of the reflection phase shift of each element is achieved by changing a specific structural parameter value of the element. Therefore, it is important to obtain the reflection phase shift curve, which changes with the element structure parameters. In order to obtain the reflection characteristics of the element, the design is analyzed by Ansys HFSS (High Frequency Structure Simulator) electromagnetic simulation software. The master-slave boundary conditions and the floquet port excitation port are used to solve the problem of an infinite period structure.

The internal structure of the element is a phoenix square loop. It provides a 360° phase range and naturally returns to its initial geometry after the phase cycle has been achieved [15]. This is the key of the phoenix principle and the

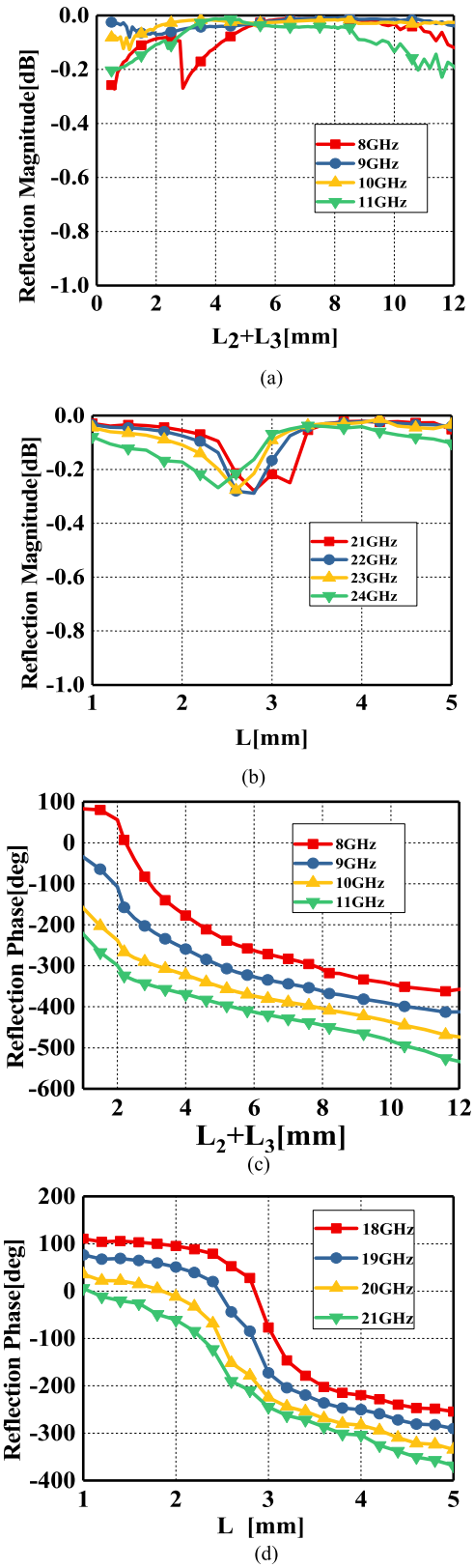

FIGURE 2. Simulation reflection magnitude curves of the element at the (a) X-band and (b) K-band. Reflection phase shift curves of one element at the (c) X-band and (d) K-band.

TABLE 1. Design parameters of the proposed element.

Parameters	L_0	L_1	L_{outer}	L_2	S	v	U
Value (mm)	1	4	5	8.5	1	2.5	6.5
Parameters	W_1	W_2	W_3	h_0	h_1	P	
Value (mm)	0.2	0.3	0.3	2	1	9	

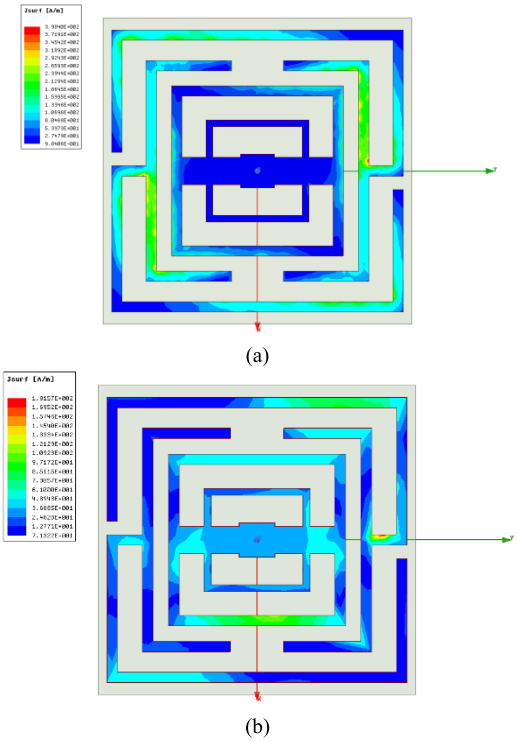

FIGURE 3. Simulation current distribution on the surface of the element structure at (a) 10 GHz and (b) 22 GHz.

explanation of its rebirth capabilities, so we call it the Phoenix element. The external structure is composed of a split square loop with two square shaped phase delay lines. The length of the square shaped phase delay lines attached to the split square loop determines the phase shift at the X- band [11]. As can be seen from Fig. 3(a) and (b), the current distribution of the element is mainly concentrated in the internal structure at 22 GHz, and in the external structure at 10 GHz.

For dual-band antennas, the most important design issue is how to suppress the interference between different bands. The internal structure corresponds to X-polarization, and the external structure corresponds to Y-polarization. Polarization isolation reduces the effects of mutual coupling between elements in dual-band, so their electrical performances hardly affect each other. The phase response curve of the element at 10 GHz with different L values is shown in Fig. 4 (a) and the phase response curve of the element at 22 GHz with different L2 + L3 values is shown in Fig. 4 (b). As can be seen from Fig. 4 (a) and Fig.4 (b), as L changes, the phase change at

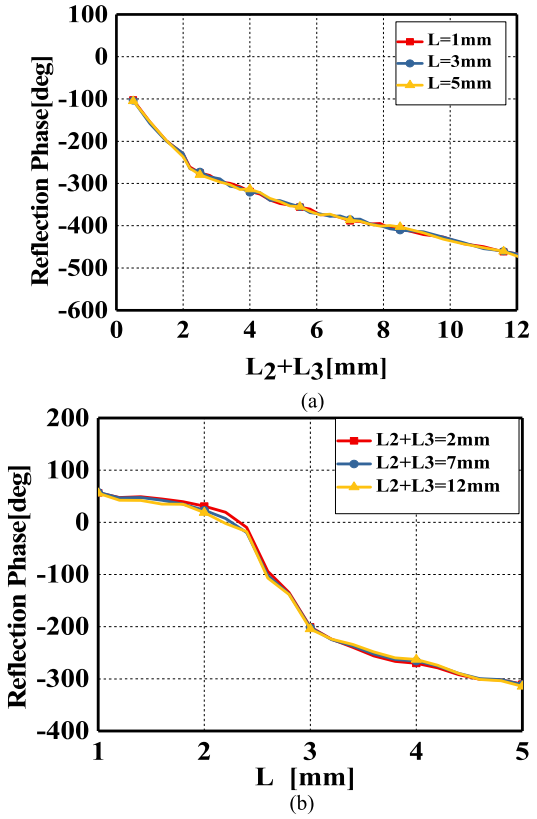

FIGURE 4. The effect of the coupling on the phase response of the element (a) Phase response at 10 GHz for different L and (b) Phase response at 22 GHz for different L2+L3.

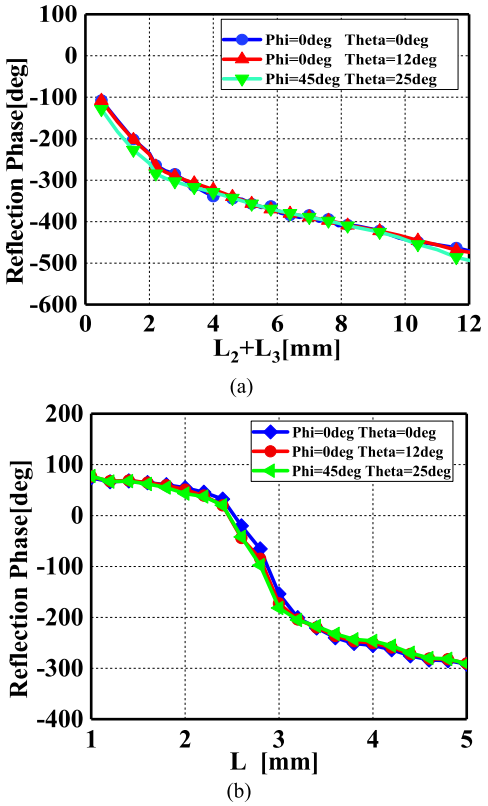

FIGURE 5. Simulation phase shift of the element at different oblique incidence angles at (a) 10 GHz and (b) 22 GHz.

10 GHz is less than 9°; the phase change at 22 GHz is less than 15° with the change of L2 + L3.Based on these results, the interference between the high band and the low band can be neglected.

C. ANALYSIS OF THE INFLUENCES OF DIFFERENT OBLIQUE INCIDENCE ANGLE

It is important to analyze the influences of different oblique incidence angles when designing a reflectarray. Considering that the focal diameter ratio (F/D) of the design is 1.2, the maximum incidence angle is less than 25°. We analyze the phase distribution of the element at different oblique incidence angles for both bands. As shown in Fig. 5(a) and (b), the element is not sensitive to the oblique incidence angles, and the phase curves exhibit little change with the incident angle at 10 GHz and 22 GHz. To simplify testing, we only consider the normal incident phase when we design this reflectarray.

III. DESIGN AND MEASUREMENT OF THE REFLECTARRAY

A. DESIGN OF THE REFLECTARRAY

It is essential to choose the proper number of elements when designing a reflectarray. For validating our design with simple processing, we select 19 × 19 elements to form the reflectarray. The overall size of the reflectarray is 200 mm×200 mm, and the space between the adjacent elements is 9 mm. In addition to the number of elements, the choice of the feed is especially important. The main requirements for the feed of the reflectarray antenna are as follows: (a) Deterministic phase center; (b) The main lobes have a small level of illumination to the edge of the array; (c) Lower cross polarization and higher power capacity. For the sake of simplicity, we use two pyramid horn antennas operating at the X-band and the K-band as the feeds. In the feed selection of the reflectarray, the incident wave is reflected to the free space after phase modulation due to the planar reflection mechanism. When the main lobe of the pattern is directly facing forward, the reflectarray using the forward-feed method is blocked by the feed resulting in an obvious decrease in radiation efficiency. As the offset-feed is more complicated, we choose the forward-feed. The feed needs to minimize the size of the feed aperture surface to avoid occlusion. In our design, the feeds are two small-diameter pyramid horn antennas operating in different bands. The horn has a size of 45 mm×37 mm at 10 GHz and 25 mm×18 mm at 22 GHz. When design a reflectarray, a proper distance between adjacent elements must be selected to avoid the occurrence of grating lobes. According to the array antenna theory, the elements' space needs to meet the following formula (1):

$$d/\lambda_0 \leq \frac{1}{1+\sin\theta} \tag{1}$$

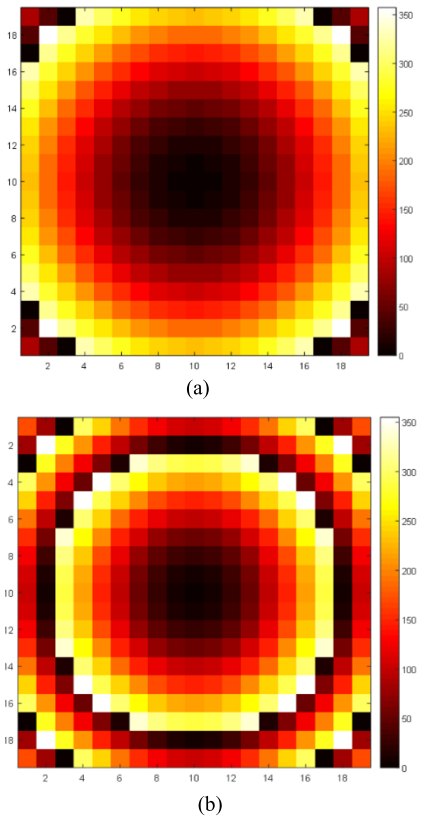

FIGURE 6. Phase distribution of each element on a reflectarray at (a) 10 GHz and (b) 22 GHz.

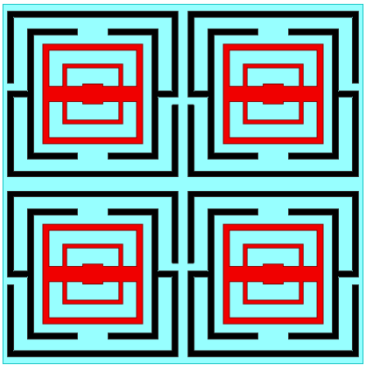

FIGURE 7. Arrangement of the elements to reduce the cross-polarization of the radiation field.

where, d is the distance between adjacent elements, θ is the angle of incidence of the feed antenna, and λ_0 is the spatial wavelength corresponding to the operating frequency.

When using a three-dimensional Cartesian coordinate system, assuming that the incident beam is directed to (θ_n, ϕ_n), the phase of reflected wave reflected by the element (located at (x_n, y_n, z_n)) is:

$$\varphi_r(x_n, y_n, z_n) = -k_0(\sin\theta_n \cos\phi_n x_n - \sin\theta_n \sin\phi_n y_n - \cos\theta_n) \quad (2)$$

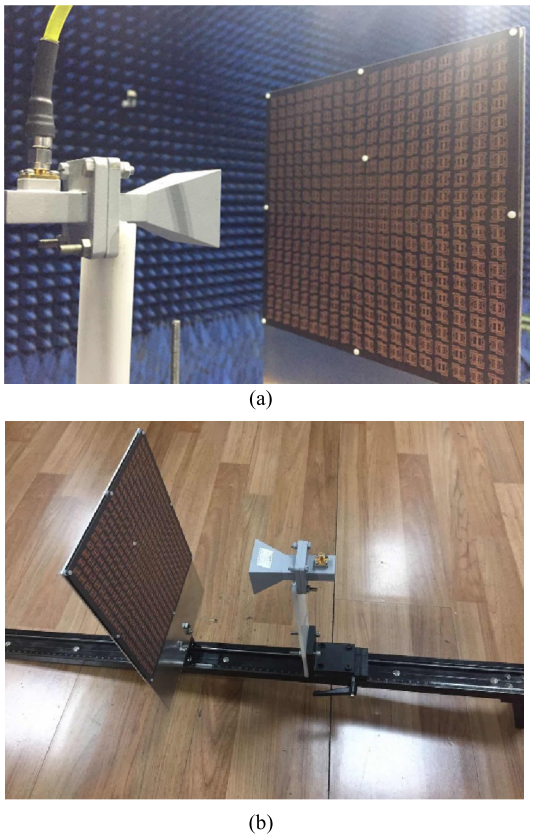

FIGURE 8. Photographs of the fabricated dual-band reflectarray antenna. (a) reflectarray prototype (b) measured in a microwave anechoic chamber.

The focal diameter ratio (F/D) is the ratio of the focal length and the largest dimension of the reflectarray. The edge of the illuminate is −10dB, so the reflectarray is designed with the F/D ratio of 1 in higher band and 1.2 in lower band respectively. We have considered the phase center of the feed antenna in the simulation, so the phase center of the feed antenna is installed 200 mm above the reflectarray in the higher band and 240 mm above the reflectarray in the lower band. The distance between the horn antenna and the reflectarray can be adjusted by the slide rail under the support frame. The phase of compensation distribution along the x-axis and direction and y-axis are completely symmetrical at 10 GHz (Fig. 2(a)) and 22 GHz (Fig. 2(b)), since the feed is located directly above the center of the reflectarray.

In a reflectarray, the path lengths from the feeds to different elements are different, which causes different phase delays generated by different location elements. In order to compensate for the phase delay caused by different paths, the reflection phase of each elements should be accurately corrected by its scattering phase shift curve. According to the formula (3):

$$\nabla L_{mn} = L_{mn} - L_{(10,10)} \quad (3)$$

where, L_{mn} is the distance from the phase center of the feed to the (m,n)th element on the reflectarray, $L_{(10,10)}$ is the distance

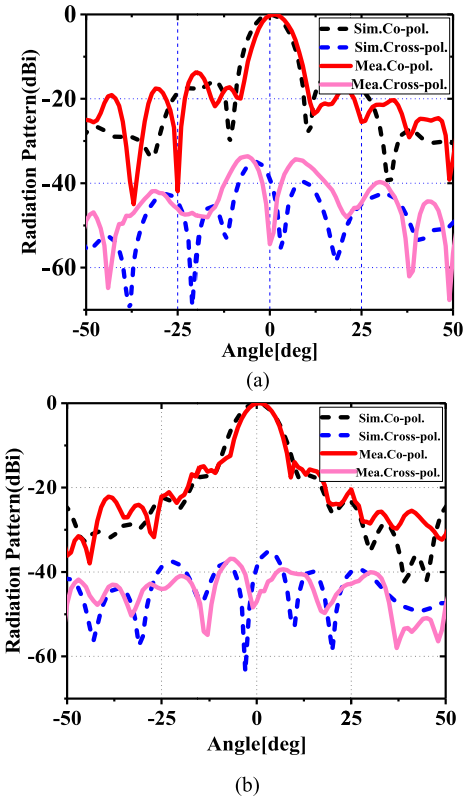

FIGURE 9. Measured and simulated radiation patterns (normalized) at 10 GHz. (a) Azimuth plane. (b) Elevation plane.

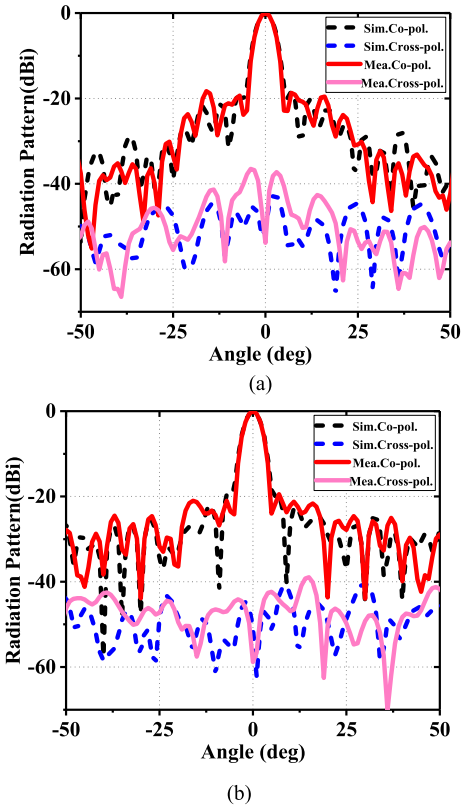

FIGURE 10. Measured and simulated radiation patterns (normalized) at 22 GHz. (a) Azimuth plane. (b) Elevation plane.

from the phase center of the feed to the center element of the reflectarray, and ∇L_{mm} is the distance from the phase center of the feed to the (m,n)th element on the reflectarray. In order to achieve high gain of the reflectarray, the phase required for the (m, n)th element is as follows:

$$\Delta\Phi_{mn} = [\Delta L_{mn}/\lambda_0 - integerof\ (\Delta L_{mn}/\lambda_0)] \times 360 \qquad (4)$$

Through the above formula, we calculate the reflection phase distribution of each element of the reflectarray as shown in Fig. 2(a) and Fig. 2(b) at 10 GHz and 22 GHz, respectively.

In order to reduce the cross-polarization of the radiation field and improve the aperture efficiency of the reflectarray, we have chosen the particular arrangement of the elements as described in [17]. The elements between the adjacent quadrants are in the mirrored arrangement as shown in Fig. 7. The cross-polarization components can cancel each other, so the cross-polarization decreases and the aperture efficiency increases.

B. MEASUREMENT OF THE REFLECTARRAY

The proposed reflectarray has been simulated and optimized by Ansoft HFSS Software. In the HFSS simulation, we can find the phase center and then let the phase center of the horn antenna and the focus of the reflectarray overlap. In the actual measurement, we keep the distance between the feed antenna and the reflection array consistent with the simulation. The antenna has been fabricated and measured, its photograph is shown in Fig. 8(a). The reflectarray consists of 361 elements on the top surface. There are some dielectric support columns between the dielectric plate and the ground; these columns are made of aluminum. The proposed prototype has been measured in a microwave anechoic chamber as shown in Fig. 8(b). The measurements and the simulation results are in good agreement as shown in Figs. 9-11.

The measured and simulated radiation patterns (normalized) at 10 GHz are shown in Fig. 9 and Fig. 10. As can be seen from the figures, the main lobe regions of the measured and simulated radiation patterns (normalized) are very similar to each other. The first sidelobe regions are slightly different between the measured and simulated radiation patterns (normalized). There are many reasons for these differences, such as the noise of the microwave anechoic chamber, the link bracket is made by aluminum, machining error, and so on. At 10 GHz, the cross polarization and sidelobe levels are lower than −30 dB and −15 dB, respectively. The cross polarization and sidelobe levels are lower than −50 dB and −19 dB at 22 GHz, respectively. For the limited space of the paper, we have only added the co-polarization patterns of the elevation pattern and the co-polarization pattern of the azimuth patterns is similar with the azimuth patterns, the simulated co-polarization patterns of the elevation

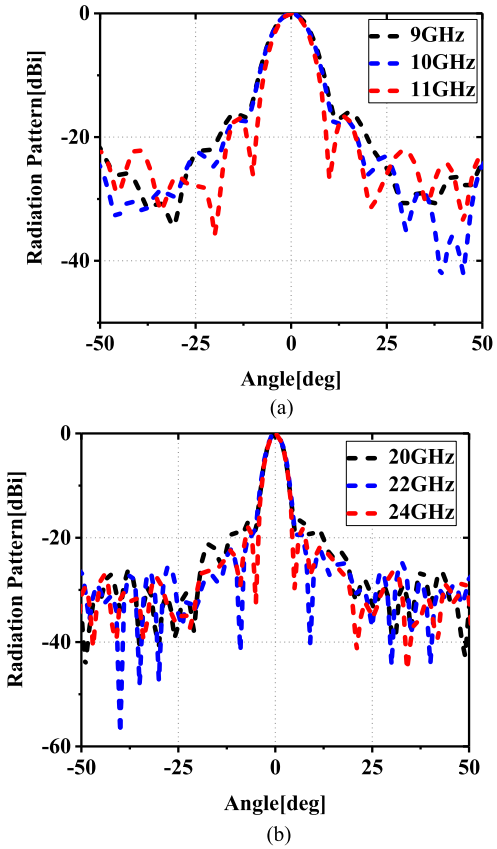

FIGURE 11. Simulated co-polarization patterns (normalized) of the elevation pattern at (a) Lower band and (b) Higher band.

TABLE 2. Comparing dual-band reflectarrays.

Reference	Frequency (GHz)	Band-Ratio (f_{higher}/f_{lower})	Measured Gain[dBi]	Aperture efficiency [%]	1-dB Gain BW [%]
This Work	10/22	2.2	23.6/30.6	41/42	20/19
[3]	8/14	1.75	18.3/22.1	29.3/27.7	-
[4]	10.2/22	2.16	26.2/29.7	47/25	16/9.1
[5]	20/30	1.5	36.7/40.0	66.5/50	-
[6]	10/15	1.5	29.1/32.6	51.3/51.1	11.5/17.5
[7]	8.5/16	1.88	22.9/28.8	40/44.8	20.7/12.9
[11]	9.7/19.2	1.98	27.7/31.8	63/42	25/18

pattern (normalized) at lower band and higher band are shown in Fig. 11. As can be seen from Fig. 12, the measured 1-dB gain bandwidths (bandwidth corresponding to 1dB less than the maximum gain) are 20% (9.1 GHz-11.1 GHz) in the X-band and 19% (19.8 GHz-23.9 GHz) in the K-band. The measured aperture efficiencies are 43% (9.5 GHz) and 44.5% (21.5 GHz) in the X-band and the K-band, respectively. The simulation and measurement results effectively demonstrate the radiation characteristics of the design. The performances compared with other single layer dual-band reflectarrays are shown in Table 2.

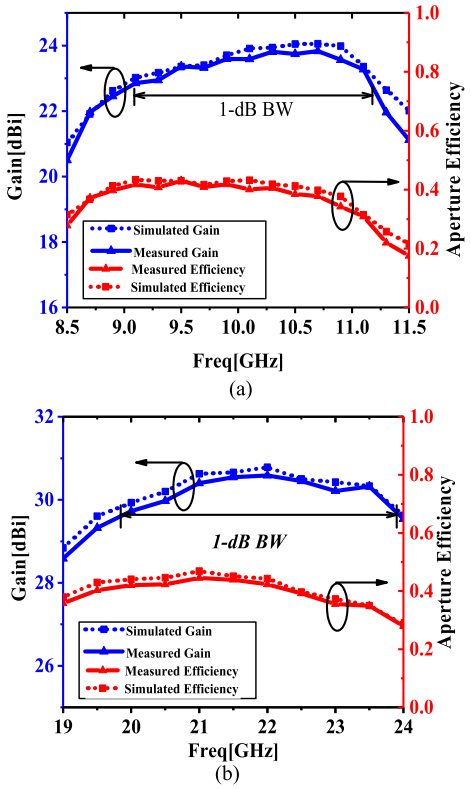

FIGURE 12. Measured and simulated gain and radiation efficiency at the (a) X-band. (b) K-band.

IV. CONCLUSION

In this paper, a single-layer dual-band wide band-ratio reflectarray with orthogonal linear polarization is designed. The novel element consists of a split square loop with two square shaped phase delay lines and a phoenix square loop; these operate at the X-band and the K-band, respectively. Through the detailed design and fabrication, the measured 1-dB gain bandwidths are 20% (9.1 GHz-11.1 GHz) in the X-band and 19% (19.8 GHz-23.9 GHz) in the K-band. The measured aperture efficiencies are 43% (9.5 GHz) and 44.5% (21.5 GHz) in the X-band and the K-band, respectively. The band-ratio of the reflectarray can reach 2.2. The proposed reflectarray is good candidate for dual-band dual-polarization wide ratio applications.

REFERENCES

[1] A. Youtz, D. Koeger, S. Reichgott, and J. Zygmaniak, "An EIA/CEA-909 compatible smart antenna system for digital terrestrial broadcasting applications," *IEEE Trans. Broadcast.*, vol. 51, no. 4, pp. 423–430, Dec. 2005.
[2] E. Martinez-de-Rioja, J. A. Encinar, M. Barba, R. Florencio, R. R. Boix, and V. Losada, "Dual polarized reflectarray transmit antenna for operation in Ku- and ka-bands with independent feeds," *IEEE Trans. Antennas Propag.*, vol. 65, no. 6, pp. 3241–3246, Jun. 2017.
[3] Y. Chen, L. Chen, H. Wang, X.-T. Gu, and X.-W. Shi, "Dual-band crossed-dipole reflectarray with dual-band frequency selective surface," *IEEE Antennas Wireless Propag. Lett.*, vol. 12, pp. 1157–1160, Sep. 2013.
[4] R. S. Malfajani and Z. Atlasbaf, "Design and implementation of a dual-band single layer reflectarray in X and K bands," *IEEE Trans. Antennas Propag.*, vol. 62, no. 8, pp. 4425–4431, Aug. 2014.

[5] R. Deng, Y. Mao, S. Xu, and F. Yang, "A single-layer dual-band circularly polarized reflectarray with high aperture efficiency," *IEEE Trans. Antennas Propag.*, vol. 63, no. 7, pp. 3317–3320, Jul. 2015.
[6] R. Deng, S. Xu, F. Yang, and M. Li, "Design of a low-cost single-layer X/Ku dual-band metal-only reflectarray antenna," *IEEE Antennas Wireless Propag. Lett.*, vol. 16, pp. 2106–2109, Apr. 2017.
[7] T. Su, X. Yi, and B. Wu, "X/Ku dual-band single-layer reflectarray antenna," *IEEE Antennas Wireless Propag. Lett.*, vol. 18, no. 2, pp. 338–342, Feb. 2019.
[8] C. Guclu, J. Perruisseau-Carrier, and O. Civi, "Proof of concept of a dual-band circularly-polarized RF MEMS beam-switching reflectarray," *IEEE Trans. Antennas Propag.*, vol. 60, no. 11, pp. 5451–5455, Nov. 2012.
[9] L. Guo, P.-K. Tan, and T.-H. Chio, "Single-layered broadband dual-band reflectarray with linear orthogonal polarizations," *IEEE Trans. Antennas Propag.*, vol. 64, no. 9, pp. 4064–4068, Sep. 2016.
[10] Z. Hamzavi-Zarghani and Z. Atlasbaf, "A new broadband single-layer dual-band reflectarray antenna in X- and ku-bands," *IEEE Antennas Wireless Propag. Lett.*, vol. 14, pp. 602–605, Nov. 2015.
[11] R. S. Malfajani and B. A. Arand, "Dual-band orthogonally polarized single-layer reflectarray antenna," *IEEE Trans. Antennas Propag.*, vol. 65, no. 11, pp. 6145–6150, Nov. 2017.
[12] M. Karimipour, N. Komjani, and I. Aryanian, "Broadband, dual-band reflectarray with dual orthogonal polarisation for single and multi-beam patterns," *IET Microw., Antennas Propag.*, vol. 13, no. 12, pp. 2037–2045, Oct. 2019.
[13] Q. Wang, Z. H. Shao, Y. J. Cheng, and P. K. Li, "Ka/W dual-band reflectarray antenna for dual linear polarization," *IEEE Antennas Wireless Propag. Lett.*, vol. 16, pp. 1301–1304, Jul. 2017.
[14] B.-Q. You, Y.-X. Liu, J.-H. Zhou, and H.-T. Chou, "Numerical synthesis of dual-band reflectarray antenna for optimum near-field radiation," *IEEE Antennas Wireless Propag. Lett.*, vol. 11, pp. 760–762, Sep. 2012.
[15] J. Zhao, T. Li, X. Cui, X. Zhao, H. Li, B. Hu, H. Wang, Y. Zhou, and Q. Liu, "A low-mutual coupling dual-band dual-reflectarray antenna with the potentiality of arbitrary polarizations," *IEEE Antennas Wireless Propag. Lett.*, vol. 16, pp. 3224–3227, Dec. 2017.
[16] L. Moustafa, R. Gillard, F. Peris, R. Loison, H. Legay, and E. Girard, "The Phoenix cell: A new reflectarray cell with large bandwidth and rebirth capabilities," *IEEE Antennas Wireless Propag. Lett.*, vol. 10, pp. 71–74, 2011.
[17] D.-C. Chang and M.-C. Huang, "Multiple-polarization microstrip reflectarray antenna with high efficiency and low cross-polarization," *IEEE Trans. Antennas Propag.*, vol. 43, no. 8, pp. 829–834, Aug. 1995.
[18] Y. Zhang, C. Cen, C. Liang, Z. Yi, X. Chen, Y. Tang, T. Yi, Y. Yi, W. Luo, and S. Xiao, "Five-band terahertz perfect absorber based on metal layer–coupled dielectric metamaterial," *Plasmonics*, vol. 14, no. 6, pp. 1621–1628, Dec. 2019.

XI LI (Member, IEEE) was born in Xian, Shaanxi, China. He received the B.S. and Ph.D. degrees in electromagnetic fields and microwave technology from Xidian University, Xi'an, China, in 2006 and 2011, respectively. He was with the Institute, from 1983 to 2003. Since 2003, he has been with Xidian University, where he is currently a Professor with the National Key Laboratory of Antennas and Microwave Technology.

His research interests include microstrip array antenna, waveguide slot array antenna, and near-field measurement.

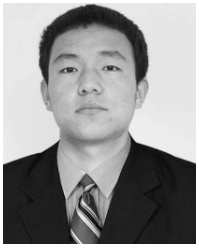

XI LI was born in Weinan, Shaanxi, China, in 1991. He received the M.S. degree in electronic and information engineering from Xidian University, Xi'an, in 2019, where he is currently pursuing the Ph.D. degree. His research interests include microstrip array antenna, reflectarray antenna, and transmitarray antennas.

LIN YANG was born in Weinan, Shaanxi, China. He received the M.S. degree in electromagnetic fields and microwave technology from Xidian University, Xi'an, China, in 1983. He was with the Institute, from 1983 to 2003. Since 2003, he has been with Xidian University, where he is currently a Professor with the National Key Laboratory of Antennas and Microwave Technology.

His research interests include antenna theory and engineering design.